Flood-Tide Deltaic Wetlands: Detection of Their Sequential Spatial Evolution

Qizhong Guo and Norbert P. Psuty

Abstract

Techniques to detect evolution of marsh islands in Great Egg Harbor Bay, New Jersey are presented in this paper. Aerial photographs and topographic maps were digitized. A geographic information system (GIS) was subsequently established with the digitized data. A computer program was also written to carry out necessary computations. Through these efforts, change in area, shift of centroid, and rotation of marsh islands were quantified. It was revealed that (1) over the recent 51-year period (1940-1991), the areal loss of the entire group of islands has amounted to slightly under 5 percent, and most individual islands have the same trends of decrease in area; (2) the centroid of the entire group of islands has shifted northeastward, 333 feet to the east and 202 feet to the north, but the trends of individual islands vary; and (3) the entire group of marsh islands has retained its general orientation through the period; however, some individual islands have rotated dramatically. These features of marsh island evolution are important to maintenance of navigation channels because they affect the width of channels between the islands and the spatial distribution of sedimentation. These features of marsh island evolution also need to be known for management of the coastal ecosystem because they are indicators of stability of biological habitats.

Introduction

Flood tide deltaic development is a dynamic element of tide-dominated barrier island systems. As noted by Hayes (1979; 1980) and Hubbard *et al.* (1979) in their geomorphological descriptions and classifications of barrier island characteristics, these flood-tide delta islands are manifestations of relative energy flows in terms of wave and tide parameters. Other formational variables, such as sediment supply and relative sea-level rise, contribute to the sequential development of deltaic forms (Boothroyd, 1985). Because the natural system of sediment supply and attendant variables are subject to a combination of systematic and random variability, case by case measurements of the spatial/temporal pattern of tidal deltaic development can establish the magnitude of the landform responses to this variability, and a comparison of these changes through time may establish the systematic direction of this variation (Kearney and Stevenson, 1991).

The areal extent of flood-tide deltas at barrier island inlets is composed of several distinctive habitats: the intertidal and supratidal wetlands, and the intertidal and subtidal shoals. These accumulations, in turn, compose islands which are bounded by distributary channels, or margins of the delta unit. It is these deltaic islands, their wetland cover and their adjacent shoals, that contain the evolutionary history of the deltaic development. Whereas the full history is obtainable only by three-dimensional analysis, aspects of the developmental history can be interpreted from the spatial distribution and shifts of the islands through time. As shown by Lyon and Greene (1992) and by Ferguson *et al.* (1993), systematic examination of aerial photographs spanning decades provides an adequate means to measure areal and spatial changes of wetland cover.

Characteristics of the Study Site

A case study approach to this problem has been conducted in the Great Egg Harbor Bay, New Jersey. Great Egg Harbor Bay (Figure 1) is part of the barrier island/backbay system that exists inland of the Holocene barrier islands and seaward of the Pleistocene mainland or upland. The bay was formed during the Holocene rise of sea level that inundated the mainland and led to the development of the barrier island chain. When sea level reached near its present elevation and achieved relative stability (approximately 0.6 mm/yr) about 3000 years ago (Psuty, 1986), the pattern of backbay flood-tide deltas (islands and marshes) was initiated. Filling in of the bay and enhancement of the flood-tide delta continued as sediment was transported inland through the Great Egg Harbor inlet. The development of marsh islands in Great Egg Harbor Bay was part of the natural flood tidal deltaic accumulation that occurred on the inland side of flood-dominated inlets where sediments were transported and distributed by the relatively high energies of the tidal exchanges. Flood-dominated deltaic shoals are common along New Jersey, indicative of the modest estuarine discharges which are insufficient to remobilize the tidally derived sedimentation and thus the buildup at the inland side of the coastal inlets.

Some estuarine sedimentation was associated with fluvial flow down the Great Egg Harbor River, but that source was limited because of the porous sandy formations in the upland and the high proportion of ground water flow rather than surface runoff (Good and Good, 1984; Martin, 1989). As described by Dobday (1981), Psuty (1986), and others, most of sediment that has accumulated in the bay has a marine source. That is, the sediments have been entering through the inlet and filling in the bay from the oceanside. This is what gives rise to the marsh islands and the shoals around

Q. Guo is in the Department of Civil and Environmental Engineering, Rutgers University, Piscataway, NJ 08855-0909.

N.P. Psuty is with the Institute of Marine and Coastal Sciences, Rutgers University, New Brunswick, NJ 08903-0231.

Photogrammetric Engineering & Remote Sensing, Vol. 63, No. 3, March 1997, pp. 273–280.

0099-1112/97/6303-273$3.00/0

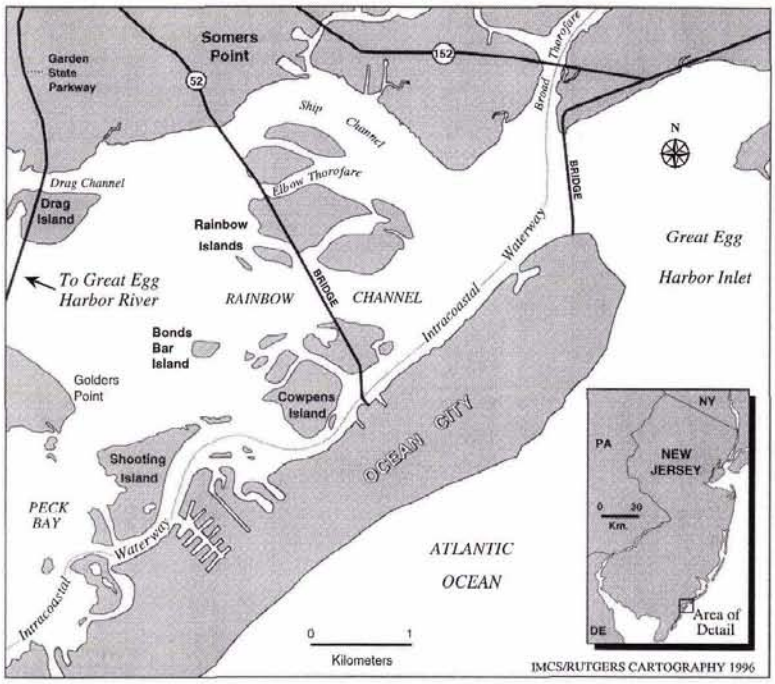

Figure 1. Great Egg Harbor Bay, New Jersey.

them. However, the supply of sediment is not infinite and it is likely that the rate of sediment input has decreased in the last few hundred years. More importantly, the rate of volumetric sediment input to the general bay area is now probably less than the rate at which the volume of the bay is increased by the current rate of sea-level rise (4 mm/yr) (Lyles *et al.*, 1988; Psuty, 1991).

Although sedimentation rates are low in the bay, there are shoal areas in the vicinity of marsh islands where sediments are accumulating under the influence of modern tidal flows and the reworking of sediments which compose the islands. There are a number of "shadow" areas to the lee of the islands where velocity and turbulence gradients are steep and sediments will accumulate naturally. There are also a number of natural channels through the islands that are kept clear by the tidal flows. The combination of the channels, the marsh-islands, and the adjacent shoals provide the pattern of flood-tide delta development. Knowledge of their spatial/temporal variation can offer insights to the process/response mechanisms that govern their geomorphological development.

Analytical Procedure

The recent spatial evolution of the flood-tide delta islands is captured on maps, charts, and aerial photographs of the area. These sources were collected and examined as the first step in establishing a comparative analysis of the varying pattern of marsh islands, adjacent shoals, and intervening channels of the flood-tide delta. Following selection of archival sources, these geomorphological features were digitized and registered to the New Jersey State Plane Coordinate System. After an evaluation of their spatial error, a series of comparisons were conducted to define the changes in marsh island and shoal positions. These data give an indication of the dynamics of the system and aid in the understanding of the morphological evolution of the flood-tide deltas. From the engineering point of view, evolution of marsh islands affects the width of channels between the islands; thus, knowledge about it is essential in terms of navigation channel maintenance. From the ecological point of view, increase or decrease of area of marsh islands will affect the availability of natural biological habitats, thus affecting the overall coastal ecosystem.

Data Sources

Aerial photographs and topographic maps of the study area were collected to provide the raw data. A complete listing of these data resources is shown in Appendix A. Aerial photos from 1940, 1963, 1981, and 1991 and topographic maps based on photos from 1950 and 1981 were used to detect the evolution of marsh islands. Other data sources, such as photomaps and nautical charts, were used as references.

Digitization and Establishment of GIS

An initial consideration of any geographical-based inquiry is the establishment of a system for recording information in a spatial matrix. Most of the encountered map data were catalogued in a latitude and longitude format. However, the more recent techniques of spatial data handling relate points on the Earth's surface to a rectangular grid system in which the ground scales of the vertical and horizontal distances are identical. The geographic referencing system chosen was the New Jersey State Plane Coordinate System that records each point in the State in units of feet from the 0/0 coordinate.

A second consideration was the compilation of all of the information in a digital, computer-compatible, spatial database, commonly referred to as a geographic information system (GIS). The GIS program PC ARC/INFO (ESRI, 1991) was chosen. Map, chart, and aerial photo data were digitized and entered into the database. Specifically, selected map and aerial photo resources were digitized for the purpose of reviewing areas of change and/or stability. Conversion of the lines on the maps and boundaries on the aerial photographs was accomplished through standard techniques identified below. The base reference map used in all of the subsequent digitization was the 1989 USGS topographic quadrangle, Ocean City, New Jersey. All registration of control points and features was accomplished with regard to the locations on this quad sheet.

Conversion Procedure: Topographic Maps

All appropriate analog map data were transferred through the use of a GTCO/DIGI-PAD digitizing table, 36- by 48-inch working area, and cursor. Coverage of the digitized area begins by selecting control points (tics) that define the boundaries and reference points. These points are recorded spatially by the system in digitizer units and are discrete locations on the digitizing table. Then, these digital units are changed to Universal Transverse Mercator coordinates (UTM) which incorporates very high spatial resolution. Later, the UTM coordinate system is replaced by the New Jersey State Plane Coordinate System, which is the system of choice for this study. Features of interest were extracted from the map by tracing the outlines of the items with the cross-hairs of the cursor. Most often the cursor was recording in "stream mode." Tracing shorelines from a topographic map is a less intensive effort than from an aerial photo because in the former the land/water boundary has been determined. Tracing with the digitizing cursor must be done carefully to retain the original juxtaposition of points represented on the map sources.

An accuracy assessment of the resulting digitized image was always employed to determine how well the positioning of the recorded data corresponded to its source. This was performed by first checking the root-mean-square (RMS) error of the control points. The RMS error is expressed mathematically as

$$\mathrm{RMS}_{\mathrm{error}} = \sqrt{\frac{e_1^2 + e_2^2 + e_3^2 + \ldots + e_n^2}{n}} \quad (1)$$

where e_i is the deviation of transformed (derived) State Plane coordinates from the original State Plane coordinates of a control point, and n is the total number of chosen control points (see next section for detail). When working in digitizer units (inches), a tolerable RMS error is in the range of 0.003 to 0.006 inches. An acceptable value of error varies depending on the accuracy of the original data, the scale of the source map, the accuracy of the digitizer, and the operator. The second accuracy assessment was conducted by checking arc alignment of lines after tracing of the entire study area was completed. An evaluation of arc alignment consists of superimposing an output product of the digitized lines onto the source map and viewing how well they trace one another.

Conversion Procedure: Aerial Photographs

Converting digitizer data from aerial photographs into the spatial coordinate system is similar to the procedure described above. However, all of the lines must be interpreted from the photos and registered to the common base. To digitize information from aerial photos, the first step is the identification of control points on the photos that can be located on photomaps incorporating the State Plane Coordinate System. These photomaps (listed in Appendix A) are rectified aerial photos with the State Plane Coordinate System superimposed that helped to identify the state plane coordinate location of particular landmarks on the aerial photographs.

Discerning marsh boundaries on an aerial photograph requires some skill because the discriminating factor is a tonal or color distinction. This is a visual evaluation, and the objective is to distinguish the precise marsh boundary. The digitization process applied to aerial photography is prone to a higher degree of error in registration and continuity than in the case of working with maps because of the continuous need to exercise judgements in the delimiting procedure. Tracing the marsh boundary on aerial photography requires more skill and patience than working with maps. But, it is possible to produce boundaries that are highly accurate.

Similar to the procedure regarding digitization from maps, features on the aerial photos are digitized in digitizer units to establish a coverage. This is done in "stream mode" to obtain many points on the shoreline while preserving the ground control points in digitizer units. Next, the State Plane coordinates of the ground control points are found from the photomaps. During the transformation, a function relating the digital units to the State Plane coordinates is established first using known coordinates (in both systems) of the ground control points. Then, digital units of the remainder of coverage's features are converted into the matrix values of the State Plane Coordinate System using the established function. The RMS error with aerial photos measures the errors between the original State Plane coordinates and the transformed State Plane coordinates of the ground control points. If the RMS error is too high, some of the ground control points are removed and the coverage is re-transformed until the RMS error meets acceptable standards.

There are two types of transformation available in the PC ARC/INFO program, affine and projective. Three or more control points are required to define the affine transformation, whereas four or more points are required to define the projective transformation. The affine transformation function is

$$x' = Ax + By + C \quad (2)$$

$$y' = Dx + Ey + F \quad (3)$$

where x and y are digitizer units of the control points, and x' and y' are the transformed State Plane coordinates of the control points. A, B, C, D, E, and F are determined by fitting the locations of control points in digital units to their corresponding original State Plane coordinates. They scale, translate, and rotate the digital units of control points.

The projective transformation is based upon a more complex function which requires a minimum of four control points: i.e.,

$$x' = \frac{Ax + By + C}{Gx + Hy + 1} \quad (4)$$

$$y' = \frac{Dx + Ey + F}{Gx + Hy + 1} \quad (5)$$

The projective transformation is only used to transform coordinates digitized directly off of high altitude aerial photography or aerial photographs of relatively flat terrain, assuming that there is no systematic distortion in the air photos.

For the aerial photographs from 1940, 1963, and 1991 (six photos) that were transformed to State Plane coordinates, an RMS error of no more than 8 feet in State Plane coordinates or 0.005 inches in digitizer units was tolerated. A projective transformation was utilized (except for the year of 1940, photo 90), rather than affine, due to the coverage being directly digitized off of the relatively high altitude photographs. An example of the errors between the original and the transformed State Plane coordinates of the chosen control points calculated in this study is shown in Table 1. Table 1 is adapted from the output of the projective transformation of photo 92, year 1940. At first, this particular coverage had nine ground control points (tics). After the initial transformations, control points 5, 6, 8, and 9 were dropped to reduce the RMS error. The calculated RMS error based on the remaining control points is 2.92 feet. To lessen the RMS error to an even greater extent, the x and y errors can be added or subtracted from values of the original State Plane coordinates and then be re-transformed.

The affine transformation was utilized for six of the total of 11 photographs (listed in Appendix A). In the case of the 1981 photographs, these were all taken at a lower altitude; therefore, an affine transformation proved to be more accurate even though the coverage was digitized directly from the

TABLE 1. ERRORS BETWEEN ORIGINAL AND TRANSFORMED STATE PLANE COORDINATES FOR CONTROL POINTS ON PHOTO 92, YEAR 1940[a]

control points	digital x (in) original x (ft)	digital y (in) original y (ft)	x error (ft)[b]	y error (ft)[c]
1	8.458	29.071		
	2017798	174582.4	−3.420987	−2.915365
2	9.646	29.124		
	2019780	174578.9	0.3015676	0.6881868
3	8.612	28.376		
	2018000	173398.0	1.176861	2.161969
4	9.187	28.214		
	2018952	173398.0	1.176861	2.161969
7	10.490	26.575		
	2021005	170281.7	−1.489211	−0.9156044

RMS error in State Plane coordinates = 2.919628 feet
RMS error in digitizer units = 0.1743862E-02 inch

[a]Adapted from output of projective transformation.
[b]x error = deviation of transformed State Plane x coordinate from the original State Plane x coordinate.
[c]y error = deviation of transformed from original y coordinates.

photograph. For the 1940 coverage (photo 90), the affine transformation was used because all of the ground control points were based in one corner of the photograph.

All of the complete aerial photo digitizations and transformations eventually had a calculated RMS error of less than 0.0025 inches, approximately 3 feet at the working map scale of 1:20,000.

Calculations Using Digitized Data

The PC ARC/INFO program has a built-in capability to calculate the surface area of the marsh islands using the digitized data. The areal values can be compared on an island by island basis as well as on the entire group of marsh islands.

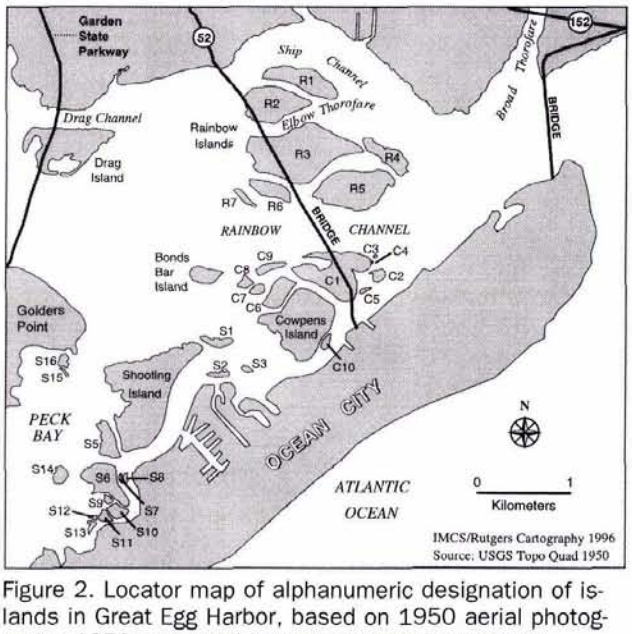

Figure 2. Locator map of alphanumeric designation of islands in Great Egg Harbor, based on 1950 aerial photography. 1950 was used because it had the greatest number of islands. Many islands are unnamed, and are therefore represented by a letter (general group) and number (within the group) sequence.

Further, additional information may be derived from a comparison of other values of the islands, such as the position of its center, length of its long axis, angle of the island, and other geometric parameters. To calculate these additional geometric parameters, a computer program independent of the GIS program was written. The written program also has the capability of calculating the surface area.

The data file was down-loaded from GIS to be used as an input data file for the written program. This data file consisted of digital data of all of the marsh islands in the study area for a particular year of interest. Each island was indexed and the boundary of each island was represented by an array of x and y coordinates. The first point in the array had the same coordinates as the last point to ensure closure of the boundary.

A numerical algorithm for integration was applied to calculate the surface area. The algorithm is expressed as follows:

$$A = -\sum_{i=1}^{N-1} \frac{y_i + y_{i+1}}{2} (x_{i+1} - x_i) \quad (6)$$

where A is the area of the individual island, and N is the total number of digital points representing the boundary. Due to the large number of digitized data points for an island, the use of simple trapezoidal integration elements produced sufficiently accurate results. The negative sign in front of the equation is necessary in the case where the data set was arranged counter-clockwise. There is no restriction on shape of island for application of this algorithm.

The centroid of the island is calculated by using the following numerical algorithm:

$$x_c = \frac{-\sum_{i=1}^{N-1} \frac{y_i + y_{i+1}}{2} (x_{i+1} - x_i) \frac{x_{i+1} + x_i}{2}}{A} \quad (7)$$

$$y_c = \frac{-\sum_{i=1}^{N-1} \frac{y_i + y_{i+1}}{2} (x_{i+1} - x_i) \frac{y_{i+1} + y_i}{2}}{A} \quad (8)$$

where x_c is the x coordinate of the centroid of the island and y_c is the y coordinate of the centroid of the island.

The angle of the island is defined by the orientation of the longest straight line across the island (long axis). Thus, the long axis is detected first, then its angle from the azimuth is calculated.

Beside the calculations of geometric parameters for the individual island, the geometric parameters for a group of islands were also computed. The total area of a group of islands was simply the sum of areas of individual islands. The centroid of the group of islands can be calculated using the same algorithm as that for the individual island, but the computational element is the individual island. The angle of the group of islands is defined differently from that of the individual island. The centroids of upper and lower half of the group of islands are located first. Then, the orientation of the straight line connecting these two centroids is defined as the angle of the group of islands.

Computational Results

Because the aerial photographic sources offered more points in the temporal scale (1940-1991) than the map/chart sources, and provided an opportunity for the initial delineation of the shoreline positions, the data comparisons are restricted to this data set, unless noted otherwise. Island designations used in this and subsequent discussions, either by number or name, are depicted in Figure 2.

TABLE 2. SUM OF AREAS OF MARSH ISLANDS

Year	1940	1963	1981	1991
Area (Ft^2)	32,034,350	32,091,070	31,180,910	30,521,460

TABLE 3. AREAL CHANGE, SHIFT OF CENTROID, AND ROTATION OF MARSH ISLANDS AS A WHOLE

Period (Yr - Yr)	Change in Area (%)	Shift of Centroid in East-Direction (ft)	Shift in Centroid in North-Direction (ft)	Rotation (+ = Clockwise) (Degrees)
1940-1963	0.177	201.3	42.7	−0.905
1963-1981	−2.836	−1.1	26.0	+0.299
1981-1991	−2.115	133.1	185.7	−0.429
1940-1991	−4.723	333.3	202.3	−1.035

Change in Area

Through the period of 51 years, the total area of the marsh islands has decreased (Table 2). After a slight increase from 1940 to 1963, the most recent trend of the change has been a decrease of just under 2 percent per decade. Over the 51-year period, the areal loss has amounted to slightly under 5 percent (Table 3).

Similar to the group trend, most individual marsh islands decreased in area over the period. Nine of the islands show a continuous loss of area (R3, R6, C8, C9, S1, S2, S5, S15, and S16), one has a persistent increase (S8), whereas the rest tend to have some variation in their areal extent, frequently increasing during the early years and decreasing more recently.

The shoals around the marsh islands were delineated on the USGS topographic maps (Appendix A). The delineated shoals were digitized and their areas were calculated. The total area of shoals increased from 12.5 million ft^2 in 1950 to 15 million ft^2 in 1981 with an increase of 20 percent.

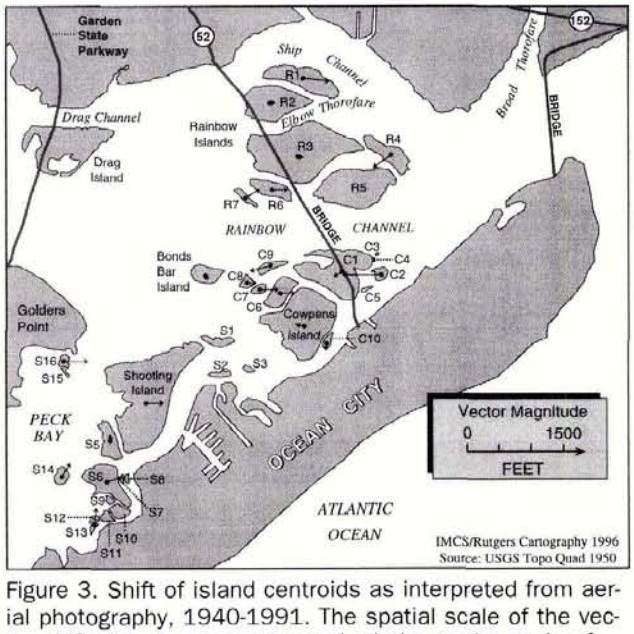

Figure 3. Shift of island centroids as interpreted from aerial photography, 1940-1991. The spatial scale of the vector shifts has been exaggerated relative to the scale of the map to permit recognition of modest changes.

Shift in Centroid

The centroid of the entire group of marsh islands has shifted northeastly, 333 feet to the east and 202 feet to the north during 1940-1991 (Table 3). The trend is consistent over the years (Table 3). The shift of the centroid of individual marsh islands from 1940 to 1991 is depicted in Figure 3. There is no persistent direction of centroid shift for the individual islands from decade to decade.

Rotation

As a group, the marsh islands have retained their general orientation (long axis azimuth) through the period, rotating 1.04 degrees in a counter-clockwise direction (Table 3). The degrees of rotation of individual marsh islands from 1940 to 1991 are shown in Table 4. Only a small number of islands show persistent direction of rotation. They are islands C6, C7, C9, and S14 in a counter-clockwise direction, and R7 and S15 in a clockwise direction.

Minimum Distance between Islands

Areal changes, shifts, and rotations of the individual islands can affect the channel widths available for flow and for navigation. Thus, minimum width distances between adjacent is-

TABLE 4. ANGLES OF MARSH ISLANDS AND THEIR CHANGES, 1940-1991

Island	Angle(40)	Angle(91)	Change
R01	101.31	101.68	0.37
R02	78.20	92.74	14.54
R03	90.10	90.39	0.29
R04	128.29	134.40	6.12
R05	78.78	77.72	−1.06
R06	115.90	119.64	3.73
R07	123.54	133.76	10.22
R08	0.00	1.18	0.00
R09	0.00	136.65	0.00
C01	82.72	80.34	−2.38
C02	129.45	43.58	−85.87
C03	142.11	0.00	0.00
C04	148.04	0.00	0.00
C05	137.22	61.98	−75.24
C06	60.74	56.63	−4.10
C07	63.96	58.53	−5.43
C08	75.00	66.19	−8.81
C09	75.82	72.81	−3.01
C10	30.22	27.15	−3.08
C11	58.37	0.00	0.00
CPS	3.92	76.49	72.57
BBR	86.79	87.31	0.53
S01	88.80	91.26	2.45
S02	60.85	90.28	29.43
S03	132.79	116.14	−16.65
S04	0.00	85.53	0.00
S05	151.52	153.80	2.28
S06	120.57	123.08	2.51
S07	53.37	0.00	0.00
S08	2.92	7.66	4.74
S09	167.72	0.00	0.00
S10	119.51	80.13	−39.37
S11	108.20	0.00	0.00
S12	0.00	0.00	0.00
S13	30.65	166.96	136.31
S14	68.73	2.01	−66.73
S15	126.30	168.28	41.98
S16	43.42	0.46	−42.96
S17	75.07	0.00	0.00
S18	62.00	0.00	0.00
S19	28.26	9.57	−18.70
STI	34.85	34.53	−0.32

lands (channel widths) were calculated to determine trends of the changes (Table 5). From Table 5, it is evident some channels are becoming significantly narrower, while other channels are becoming wider or retaining a similar width. It was determined that over the 51 years Rainbow Channel between R4 and C1 became 8 percent narrower, the channel between Bonds Bar Island and C8 became 36 percent wider, whereas the western inlet (between C1 and C6) to Little Finger Channel became 4 percent wider and the channel itself (between C1 and Cowpens Island) became 4 percent narrower.

Evolution of Marsh Islands as Sub-Groups

Another approach in evaluating the changes of the islands through time is to look at sub-groups of islands and determine whether some portions of the total system are more dynamic than others. An initial separation of the marsh islands produced a division into three groups. These three groups are (1) north group, (2) south group, and (3) southwest group. The islands in the north group include R1, R2, R3, R4, R5, R6, R7, R8, and R9 (Figure 2). The islands in the south group include C1, C2, C3, C4, C5, C6, C7, C8, C9, C10, C11, Cowpens Island, and Bonds Bar Island (Figure 2). The southwest group includes S1, S2, S3, S4, S5, S6, S7, S8, S9, S10, S11, S12, S13, S14, S15, S16, S17, S18, S19, and Shooting Island (Figure 2). Table 6 shows the change in area, shift of centroid, and rotation of the three groups of islands from 1940 to 1991.

The data show that the major reduction in surface area occurred in the southwest group of islands, that all three groups of islands shifted eastward (northeast or southeast), and that both the north and south groups of islands rotated clockwise whereas the southwest group retained essentially the same orientation. The areas of adjacent shoals were also calculated as three groups. The sum of areas of shoals around the islands in the north group decreases 45 percent from 1950 to 1981, that in the south group increases 0.98 percent, and that in the southwest group increases 484 percent. It is noted that the north group of islands is losing island area as well as shoal area around the islands, the south group has small gains in both island and shoal, and the southwest group is changing from an island habitat to a shoal habitat.

TABLE 5. MINIMUM DISTANCE (FT) BETWEEN MARSH ISLANDS, 1940-1991

Islands	1940	1963	1981	1991
R3 - R4	113.7	112.2	84.9	60.2
R4 - R5	233.4	70.5	33.6	17.7
R4 - R6	3231.9	3157.4	3023.9	3007.1
C1 - C2	419.2	145.5	58.6	80.9
C8 - C9	320.9	314.2	224.4	236.3
C7 - C9	312.5	274.0	270.7	259.3
CPS - C10	79.2	35.3	37.6	29.0
R4 - C1	3323.7	2659.7	3076.0	3063.6
R3 - R6	216.3	238.1	295.4	324.0
R6 - R7	337.6	345.7	429.8	434.4
C7 - C8	100.7	74.2	139.0	144.1
C1 - C9	273.3	270.4	463.4	523.4
BBR - C8	670.0	772.2	917.7	907.4
CPS - S3	1402.8	1353.7	1497.8	1522.8
R1 - R2	197.8	139.6	186.9	200.0
R1 - R3	922.5	912.2	918.7	905.7
R2 - R3	415.7	410.3	380.7	464.3
R3 - R5	258.5	238.7	222.4	265.8
C1 - CPS	256.5	292.3	244.6	245.4
C1 - C6	268.2	233.8	302.6	279.4
C6 - C7	197.8	146.5	211.8	199.0
C6 - CPS	96.2	95.0	101.1	97.3
C6 - C9	379.9	297.4	345.8	363.9

TABLE 6. AREAL CHANGE, SHIFT OF CENTROID, AND ROTATION OF MARSH ISLANDS AS THREE GROUPS, 1940-1991

Group	Change in Island Area (%)	Shift of Centroid in East-Direction (ft)	Shift of Centroid in North-Direction (ft)	Rotation (+ Clockwise) (degree)
North	−1.94	179.0	47.1	+7.54
South	0.76	139.6	35.8	+17.74
Southwest	−13.04	174.3	−39.8	−0.28

TABLE 7. AREAL CHANGE, SHIFT OF CENTROID, AND ROTATION OF MARSH ISLANDS AS TWO GROUPS FROM 1940-1991

Group	Change in Area (%)	Shift of Centroid in East-Direction (ft)	Shift of Centroid in North-Direction (ft)	Rotation (+ Clockwise) (degree)
East	−0.95	162.6	8.7	+0.40
West	−13.04	174.3	−39.8	−0.28

A second separation is to divide the marsh islands into two groups, east and west. The east group includes the north and the south groups in Table 6, and the west group is the same as the southwest group in Table 6. The data in Table 7 show that the east group continues to decrease in area while shifting eastward, whereas the other changes are minor. Correspondingly, the sum of areas of shoals in the east group decreases by 34.6 percent from 1950 to 1981, and that from west group increases by 484 percent.

Interpretations of Computational Results

One aspect of sedimentation dynamics is derived from the spatial movement, migration, or rotation of the marsh islands near the inlet of Great Egg Harbor. If island shifts were sufficiently large to be recorded between revisions of the topographic maps, this would be evidence of changing sedimentation and sedimentation patterns. Further, if the channels were changing and these changes were noted on the maps and charts, this would be additional evidence of shifts in the sedimentation and sedimentation patterns. Aerial photography conducted over the area through a period of 1940-1991 provides visual evidence of 51 years of shoreline, channel, shoal, and island stability/instability.

The horizontal migration/stability of the marsh islands has importance in evaluating the permanence of navigation channels. Channels which are narrowing rapidly may be silting at a high rate. Islands that are shifting or rotating may represent selective transfers of sediment and thus point to trends in sedimentation and sedimentation patterns.

Comparison of the topographic maps as well as the aerial photographs indicates that the marsh islands are losing area, and that, except for the southwestern area, the gain in tidal shoals does not compensate for the loss. This is in keeping with most other estuarine wetlands that are being reduced in surface area as sea level rises globally (Psuty, 1992; Kearney and Stevenson, 1991). The loss is associated with a low sediment input that is not capable of providing the mass needed to maintain volume equilibrium during the rise in sea level. Thus, there is evidence that the general rate of sediment input is lower than the rate of sea-level rise for this portion of New Jersey.

Island spatial shifts (measurements of centroid displacements) may be in response to the loss in area but they are also due to the counter-clockwise flow pattern and accompanying sediment transfers (Psuty *et al.*, 1993). A higher proportion of water flows through Ship Channel (56 percent of

the peak flow rate) than the Intracoastal Waterway (16 percent of the peak flow rate) during the flood tide. During the ebb tide, 38 percent of the peak flow exits through the Ship Channel and 34 percent through the Intracoastal Waterway. Island shifts are driven by the exposure of the island edges, by the sediment transfers, and by the sheltered locations for sediment settling and accumulation. Island shifts show the pattern of sedimentation and especially show the net direction of sediment transfers around the islands. This has considerable importance in determining impacts of dredged channels in the vicinities of the islands.

The data on island rotation are inconclusive. The small net change in orientation of the long axis of the island groups is within measurement error and there seems to be no consistent trend.

Conclusions

Estuarine systems are the product of the Holocene changes in sea level and the variable availability of sediment supplied to them from continental and marine sources. The development of wetlands and their maximum spatial extent marks the past few thousand years when sea-level rise has been relatively slow. However, with the recent accelerated rise of sea level and the decreasing rate of sediment supply, many of the estuarine wetlands are being reduced in dimension. Part of the change is affecting the marsh islands in the flood-tide deltas developed at the inlets of barrier islands leading into the estuarine systems. There has been a spatial response of form, area, and orientation of these marsh islands. Where adequate aerial photo coverage and topographic maps exist, there is the opportunity to interpret, digitize, and fit images in a GIS format and to establish the magnitude and distribution of the spatial responses.

As demonstrated from an analysis of the marsh islands in the flood-tide delta of the Great Egg Harbor estuary, there are measurable spatial shifts and dimensional changes within the past 51 years. The areal loss of the entire group of islands has amounted to slightly under 5 percent. The centroid of the entire group of islands has shifted 333 feet to the east and 202 feet to the north. The entire group of marsh islands has retained its general orientation through the period; however, some individual islands have rotated dramatically. Knowledge of the magnitude and direction of the change is fundamental to the understanding of the functioning of the estuarine system and that, in turn, is critical to the subsequent management of the estuarine systems and the many cultural practices that exist within estuaries.

Acknowledgments

Support for this study was provided by O'Dea, Pavlo & Associates, Inc., New Hyde Park, New York. Davis Harris carried out the digitization work, and Michael Siegel assisted in the production of the figures.

References

Boothroyd, J.C., 1985. Tidal inlets and tidal deltas, *Coastal Sedimentary Environments*, 2nd Edition (R.A. Davis, editor), Springer-Verlag, New York, pp. 445–532.

Dobday, M.P., 1981. *The Holocene Geologic History of the Great Egg Harbor River Estuary*, M.A. Thesis, Temple University, Philadelphia, Pennsylvania, 200 p.

ESRI (Environmental Systems Research Institute), 1991. *PC ARC/INFO Starter Kit User's Guide*, Redland, California.

Ferguson, R.L., L.L. Wood, and D.B. Graham, 1993. Monitoring spatial change in seagrass habitat with aerial photography, *Photogrammetric Engineering & Remote Sensing*, 59:1033–1038.

Good, R.E., and N.F. Good, 1984. The Pinelands National Reserve: An ecosystem approach to management, *Bioscience*, 34:169–173.

Hayes, M.O., 1979. Barrier island morphology as a function of tidal and wave regime, *Barrier Islands: From the Gulf of St. Lawrence to the Gulf of Mexico* (S.P. Leatherman, editor), Academic Press, New York, pp. 1–27.

———, 1980. General morphology and sediment patterns in tidal inlets, *Sedimentary Geology*, 26:139–156.

Hubbard, D.K., G. Oertel, and D. Nummedal, 1979. The role of waves and tidal currents in the development of tidal-inlet sedimentary structures and sand body geometry: Examples from North Carolina, South Carolina and Georgia, *Journal of Sedimentary Petrology*, 49:1073–1092.

Kearney, M.S., and J.C. Stevenson, 1991. Island land loss and marsh vertical accretion rate evidence for historical sea-level changes in Chesapeake Bay, *Journal of Coastal Research*, 7:403–416.

Lyles, S.D., L.E. Hickman, and H.A. Debaugh, Jr., 1988. *Sea Level Variations for the United States*, Office of Oceanography and Marine Assessment, National Oceanic and Atmospheric Administration, Washington, D.C., 182 p.

Lyon, J. G., 1992. Use of aerial photographs to measure the historical areal extent of Lake Erie coastal wetlands, *Photogrammetric Engineering & Remote Sensing*, 58:1355–1360.

Martin, M., 1989. *Ground Water Flow in the New Jersey Coastal Plain*, U.S. Geological Survey Open File Report 87-528, West Trenton, New Jersey.

Psuty, N.P., 1986. Holocene sea-level in New Jersey, *Physical Geography*, 7:154–167.

———, 1991. *The Effects of an Accelerated Rise in Sea Level on the Coastal Zone of New Jersey, U.S.A.*, A report to the Governor's Science Advisory Committee, Contribution 91-55, Institute of Marine and Coastal Sciences, Rutgers University, New Brunswick, New Jersey, 51 p.

———, 1992. Estuaries: Challenges for Coastal Management, *Ocean Management in Global Change* (P. Fabbri, editor), Elsevier Applied Science, London, pp. 502–520.

Psuty, N.P., Q. Guo, and N.S. Suk, 1993. *Sediments and Sedimentation in the Proposed ICWW Channels, Great Egg Harbor Bay, New Jersey*, Final Report, Rutgers University, New Brunswick, New Jersey, 107 p. + 4 Appendices.

(Received 3 March 1995; accepted 17 July 1995; revised 14 February 1996)

Appendix A

Aerial Photographs, Maps, and Charts Covering Marsh Islands in Great Egg Harbor Bay

A. Aerial Photographs

1. **1940**/February 26/black-white/9" × 9"/Intera Information Technology/1:20000/flight line #7, photos 04, 90, and 92.

2. **1963**/June 23/black-white/9" × 9"/USDA-Agricultural & Conservation Stabilization Service/1:20000/photos EAQ-1DD-9 and 11.

3. **1981**/February 13/black-white/36" × 36"/U.S. Geological Survey/1:3500/Project VFBE, photos 3-4, 3-6, 3-212, 3-217, and 4-7.

4. **1991**/March 11/black-white/36" × 36"/U.S. Geological Survey/1:10000/National Aerial Photography Program/photo 2994-42.

B. Topographic Maps

1. **1989.** Ocean City, NJ, 7.5-minute topographic quadrangle, U.S. Geological Survey, scale 1:24000, based on 1981 aerial photography.

2. **1952.** Ocean City, NJ, 7.5-minute topographic quadrangle, U.S. Geological Survey, scale 1:24000, based on 1950 aerial photography.

3. **1952.** Marmora, NJ, 7.5-minute topographic quadrangle, U.S. Geological Survey, scale 1:24000, based on 1950 aerial photography.

C. Photo Maps*

1. **1977,** July 19. Cowpens Island, Ocean City, N.J., State of N.J. Department of Environmental Protection, 1:2400, #161-2022.

2. **1977,** August 19. Bonds Bar Island, Ocean City, N.J., State of N.J. Department of Environmental Protection, 1:2400, #161-2016.

3. **1977,** August 29. Rainbow Thorofare, Ocean City, N.J., State of N.J. Department of Environmental Protection, 1:2400, #168-2022.

4. **1978,** July 29. Elbow Thorofare, Ocean City, N.J., State of N.J. Department of Environmental Protection, 1:2400, #168-2016.

5. **1986,** March. Photoquad of Ocean City, N.J., State of N.J. Department of Environmental Protection, 1:24000, #167.

*All photomaps were prepared for the State of New Jersey Department of Environmental Protection (Office of Environmental Analysis) by the MARK HURD Corporation.

D. Nautical Charts

1. **1986,** November 15. 23rd Edition, Little Egg Harbor to Cape May, NJ: Intracoastal Waterway, National Oceanic and Atmospheric Administration-National Ocean Service, scale 1: 40,000, Nautical Chart #12316.

Forthcoming Articles

Georges Blaha, *Accuracy of Plates Calibrated by an Automatic Monocomparator.*

Gerardo Bocco *and* Hugo Riemann, *Quality Assessment of Polygon Labeling.*

Michel Boulianne, Clément Nolette, Jean-Paul Agnard, *and* Martin Brindamour, *Hemispherical Photographs Used for Mapping Confined Spaces.*

L. Bruzzone, C. Conese, F. Maselli, *and* F. Roli, *Multisource Classification of Complex Rural Areas by Statistical and Neural-Network Approaches.*

Frank Canters, *Evaluating the Uncertainty of Area Estimates Derived from Fuzzy Land-Cover Classification.*

Russell G. Congalton, *Exploring and Evaluating the Consequences of Vector to Raster and Raster to Vector Conversion.*

Ronald J. Duhaime, Peter V. August, *and* William R. Wright, *Automated Vegetation Mapping Using Digital Orthophotography.*

Christopher D. Elvidge, Kimberly E. Baugh, Eric A. Kihn, Herbert W. Kroehl, *and* Ethan R. Davis, *Mapping City Lights with Nighttime Data from the DMSP Operational Linescan System.*

Patricia G. Foschi *and* Deborah K. Smith, *Detecting Subpixel Woody Vegetation in Digital Imagery Using Two Artificial Intelligence Approaches.*

Clyde C. Goad *and* Ming Yang, *A New Approach to Precision Airborne GPS Positioning for Photogrammetry.*

Luoheng Han, *Spectral Reflectance with Varying Suspended Sediment Concentrations in Clear and Algae-Laden Waters.*

Perry J. Hardin *and* J. Matthew Shumway, *Statistical Significance and Normalized Confusion Matrices.*

Robert L. Huguenin, Mark A. Karaska, Donald Van Blaricom, *and* John R. Jensen, *Subpixel Classification of Bald Cypress and Tupelo Gum Trees in Thematic Mapper Imagery.*

Ronald E. Huss *and* Mark A. Pumar, *Effect of Database Errors on Intervisibility Estimation.*

Kazuo Kobayashi *and* Chuji Mori, *Relations between the Coefficients in Projective Transformation Equations and the Orientation Elements of a Photograph.*

Miklos Kovats, *A Large-Scale Aerial Photographic Technique for Measuring Tree Heights on Long-Term Forest Installations.*

Rongxing Li, *Mobile Mapping—An Emerging Technology for Spatial Data Acquisition.*

D.D. Lichti *and* M.A. Chapman, *Constrained FEM Self-Calibration.*

Hans-Gerd Maas *and* Thomas Kersten, *Aerotriangulation and DEM/Orthophoto Generation from High Resolution Still-Video Imagery.*

Scott Mason, *Heuristic Reasoning Strategy for Automated Sensor Placement.*

Justin D. Paola *and* Robert A. Schowengerdt, *The Effect of Neural Network Structure on a Multispectral Land-Use/Land-Cover Classification.*

Robert Riou *and* Frédérique Seyler, *Texture Analysis of Tropical Rain Forest Infrared Satellite Images.*

A.K. Skidmore, B.J. Turner, W. Brinkhof, *and* E. Knowles, *Performance of a Neural Network: Mapping Forests Using GIS and Remotely Sensed Data.*

Youngsinn Sohn *and* Roger M. McCoy, *Mapping Desert Shrub Rangeland Using Spectral Unmixing and Modeling Spectral Mixtures with TM Data.*

David M. Stoms, Michael J. Bueno, *and* Frank W. Davis, *Viewing Geometry of AVHRR Image Composites Derived Using Multiple Criteria.*

Lucien Wald, Thierry Ranchin, *and* Marc Mangolini, *Fusion of Satellite Images of Different Spatial Resolutions: Assessing the Quality of Resulting Images.*

James D. Wickham, Robert V. O'Neill, Kurt H. Ritters, Timothy G. Wade, *and* K. Bruce Jones, *Sensitivity of Selected Landscape Pattern Metrics to Land-Cover Misclassification and Differences in Land-Cover Composition.*

Paul A. Wilson, *Rule-Based Classification of Water in Landsat MSS Images Using the Variance Filter.*

Ding Yuan, *A Simulation Comparison of Three Marginal Area Estimators for Image Classification.*